



**HAL**  
open science

# An efficient Nb-modified BiVO<sub>4</sub> film for photo-induced bacterial inactivation and photocatalytic removal of organic pollutants

Olivier Monfort, Ewa Dworniczek, Leonid Satrapinsky, Alicja Seniuk, Daniela Nyblova, Gustav Plesch

## ► To cite this version:

Olivier Monfort, Ewa Dworniczek, Leonid Satrapinsky, Alicja Seniuk, Daniela Nyblova, et al.. An efficient Nb-modified BiVO<sub>4</sub> film for photo-induced bacterial inactivation and photocatalytic removal of organic pollutants. *New Journal of Chemistry*, 2018, 42 (8), pp.5664-5667. 10.1039/c8nj01069b . hal-01807089

**HAL Id: hal-01807089**

**<https://univ-rennes.hal.science/hal-01807089>**

Submitted on 19 Jul 2018

**HAL** is a multi-disciplinary open access archive for the deposit and dissemination of scientific research documents, whether they are published or not. The documents may come from teaching and research institutions in France or abroad, or from public or private research centers.

L'archive ouverte pluridisciplinaire **HAL**, est destinée au dépôt et à la diffusion de documents scientifiques de niveau recherche, publiés ou non, émanant des établissements d'enseignement et de recherche français ou étrangers, des laboratoires publics ou privés.

# Efficient Nb-modified BiVO<sub>4</sub> film for photo-induced bacterial inactivation and photocatalytic removal of organic pollutant

Olivier Monfort,<sup>\*ab</sup> Ewa Dworniczek,<sup>c</sup> Leonid Satrapinsky,<sup>d</sup> Alicja Seniuk,<sup>c</sup> Daniela Nyblova<sup>a</sup> and Gustav Plesch<sup>a</sup>

<sup>a</sup>Comenius University in Bratislava, Faculty of Natural Sciences, Department of Inorganic Chemistry, 842 15 Bratislava, Slovakia

<sup>b</sup>Univ Rennes, Ecole Nationale Supérieure de Chimie de Rennes, CNRS, ISCR (Institut des Sciences Chimiques de Rennes) – UMR 6226, F-35000 Rennes, France

<sup>c</sup>Wroclaw Medical University, Department of Microbiology, 50368 Wroclaw, Poland

<sup>d</sup>Comenius University in Bratislava, Faculty of Natural Sciences, Department of Comenius University in Bratislava, Faculty of Mathematics Physics and Informatics, Department of Experimental Physics, 842 48 Bratislava, Slovakia.

\*Correspondence: [olivier.monfort@ensc-rennes.fr](mailto:olivier.monfort@ensc-rennes.fr)

## Abstract

Using Nb-modified BiVO<sub>4</sub> film, the photo-induced properties in Methicillin-resistant *Staphylococcus aureus* (MRSA) inactivation under simulated solar light reached 43% after 1 hour irradiation while 72% of Rhodamine B was degraded after 3 hours. To evaluate the efficiency of Nb-BiVO<sub>4</sub>, its photo-performance was compared with that of BiVO<sub>4</sub>/TiO<sub>2</sub> composites and pure BiVO<sub>4</sub>.

## Introduction

Bismuth vanadate (BiVO<sub>4</sub>) is a promising solar-light driven photocatalyst which exhibits energy band gap at 2.4 eV.<sup>1,2</sup> For this reason BiVO<sub>4</sub> materials, and more generally Bi-based oxide materials, are intensively studied for photodegradation of organic pollutant and photoproduction of O<sub>2</sub> by water splitting.<sup>1-6</sup> However BiVO<sub>4</sub> photocatalyst exhibits high recombination rate of electron-hole pairs that limits its performance.<sup>1,2</sup> Therefore it is necessary to modify BiVO<sub>4</sub> photocatalyst to increase its efficiency in photochemical processes by designing doped or composite systems.<sup>1,2</sup> Modification using silver or carbon-based materials can be cited.<sup>3-6</sup>

On the other hand, BiVO<sub>4</sub>-based photocatalysts are mainly studied in the form of powder suspensions<sup>7-10</sup> rather than supported systems<sup>11-15</sup> for photo-oxidative degradation of organic pollutant. Supported systems such as films are more practical for obvious reason: the readily post-separation of the photocatalyst with the polluted media.<sup>16</sup> Different photocatalytic mechanisms were reported according to the way of BiVO<sub>4</sub> modification. Indeed variously doped and numerous BiVO<sub>4</sub> composite systems could

exhibit either photogenerated holes or radicals as main oxidative species.<sup>3-11,15</sup> In addition, among the works devoted to photo-induced antimicrobial properties of bismuth vanadate-based materials, most of them are focused on *E. coli* inactivation.<sup>17-26</sup>

In this work, bismuth vanadate films are prepared by metal organic decomposition and modified using niobium(V) and TiO<sub>2</sub>. The photocatalytic efficiency in Rhodamine B degradation was compared using different BiVO<sub>4</sub>-based films and the study of inactivation of MRSA strain is, for the first time, demonstrated under solar-like irradiation. MRSA (Methicillin-resistant *Staphylococcus aureus*) are chosen in this study because such bacteria are clinically important and more resistant than *E. coli* bacterial strains. Indeed, the *Staphylococcus aureus* is the most common bacterial pathogen worldwide.<sup>27</sup> Its methicillin-resistant variants (MRSA) generate serious concern over the loss of antibiotics susceptibility.<sup>27</sup> The observed photo-induced properties as well as mechanisms are also discussed here, especially for Nb-modified BiVO<sub>4</sub>. Such photocatalytic films could find promising environmental applications but also could be developed for clinical or food technology.

## Experimental

Pure bismuth vanadate films were prepared using a precursor solution based on vanadium(IV) acetylacetonate and bismuth(III) nitrate pentahydrate.<sup>13,14</sup> For the preparation of Nb-BiVO<sub>4</sub>, the precursor solution was modified by 10 at% of Nb(V) chloride while BiVO<sub>4</sub>/TiO<sub>2</sub> composites were prepared using the BiVO<sub>4</sub> precursor solution and a TiO<sub>2</sub> sol-gel.<sup>13,14</sup> Films were deposited using doctor blade method by casting the precursor solution between Scotch® tape using glass Pasteur pipette on Si/SiO<sub>2</sub> substrates. Crystalline films were obtained after subsequent metal organic decomposition at 500°C for 5 minutes. For the composites, two different layered configurations were designed: top coated-BiVO<sub>4</sub> over TiO<sub>2</sub> (top-BiVO<sub>4</sub>/TiO<sub>2</sub>) and top coated-TiO<sub>2</sub> over BiVO<sub>4</sub> (top-TiO<sub>2</sub>/BiVO<sub>4</sub>). The films were approximatively 1 µm thick.

The composition of crystalline phases in the films was analyzed by X-ray diffraction using PANalytical XPert Pro MRD diffractometer. The surface morphology was characterized by scanning electron microscopy using Tescan Lyra III. The energy band gap was evaluated by diffuse reflectance spectroscopy using Shimadzu model 2600 spectrophotometer.

Photocatalytic experiments were performed for 180 minutes under solar-like irradiation using a B-class solar simulator with spectral characteristics similar to natural sunlight (HQI TS – OSRAM 400 W;  $\lambda_{max} = 525$  nm) where the decolorization of 10<sup>-5</sup> M Rhodamine B (RhB) solution was followed by UV-vis

spectrophotometer (Jasco V-530). The mechanism of photooxidative degradation was determined indirectly using charge scavengers of the different species possibly involved: ammonium oxalate for photogenerated holes ( $h^+$ ), iso-propanol for hydroxyl radicals ( $OH^\bullet$ ) and p-benzoquinone for superoxide radicals ( $O_2^{\bullet-}$ ). The experiments were performed in triplicates.

To evaluate the antimicrobial effectiveness at the surface of the samples, modified *JIS Z 2801: 2010* test method, was used. Briefly, 100  $\mu$ L of MRSA K324 which represents (at  $t = 0$  min)  $3 \cdot 10^5$  CFU/mL (Colony Forming Unit) was instilled onto each  $BiVO_4$ -based film (1  $cm^2$ ) kept in a humid atmosphere to avoid extensive drying of the suspension and irradiated for 30 min and 60 min (Xenon lamp – 15  $mW/cm^2$ ). Control experiments were carried out in the dark, under the same conditions. At appropriate time, the test bacteria were washed out with sterile saline solution, to release the inoculum from the surface. Quantification of the viable cells was performed by a standard plating method and incubation at 37°C for 24-48h. Bactericidal activity of the samples was evaluated using logarithmic reduction of number of microbial cells. Each antimicrobial test was performed in duplicate.

## Results and discussion

The crystalline phase composition of freshly prepared materials is analyzed by XRD (Electronic Supplementary Information). All the photocatalysts exhibit crystalline monoclinic scheelite  $BiVO_4$  structure (PDF 00-014-0688). In addition, no other phase is detected in Nb- $BiVO_4$  indicating that niobium is probably present in the form of oxide either amorphous or at nanosize level. This observation is confirmed by EDX (Energy Dispersive X-ray Spectroscopy) measurement which detected niobium in Nb- $BiVO_4$  sample. Both  $BiVO_4/TiO_2$  composites exhibit additional anatase phase (PDF 00-021-1272). The energy band gap of pure and Nb-modified  $BiVO_4$  is evaluated at 2.4 eV approximately for both materials by using the Tauc's method, i.e. they absorb light in the visible region (at  $\lambda \leq 500$  nm). However, the composites exhibited a blue shift in the energy band gap (2.5 eV) due to screening effect of  $TiO_2$  that is absorbing only in the UV region.

Strong differences appear in the morphology of film surface. In Fig. 1, it is clear that Nb- $BiVO_4$  (Fig. 1c) exhibits a porous surface morphology presenting a hierarchical structure while pristine and composite samples (Fig. 1a,b) have a more dense and homogeneous surface. Concerning the both composites, top- $BiVO_4/TiO_2$  sample exhibits similar morphology than pure  $BiVO_4$  (Fig. 1a) while top- $TiO_2/BiVO_4$  has similar surface than pure  $TiO_2$  (Fig. 1b).

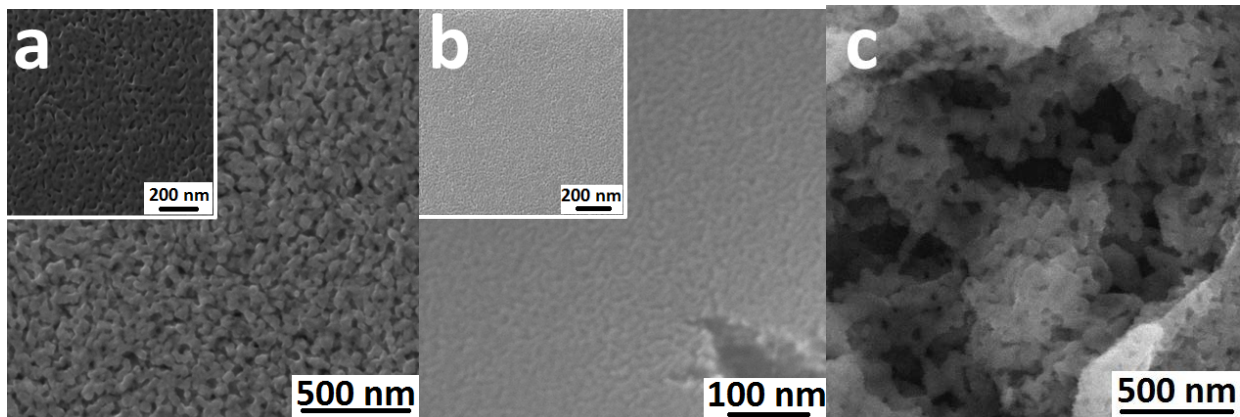


**Figure 1.** Surface morphology of (a) pristine  $\text{BiVO}_4$  and (inset) top-coated  $\text{BiVO}_4$  over  $\text{TiO}_2$  composite, (b) pure  $\text{TiO}_2$  and (inset) top-coated  $\text{TiO}_2$  over  $\text{BiVO}_4$  composite and (c)  $\text{Nb-BiVO}_4$ .

The photocatalytic degradation of RhB was followed under simulated solar irradiation and the corresponding degradation rates are presented in Fig. 2. It is worth to notice that the photocatalysts remain intact after their use since XRD patterns did not change (Electronic Supplementary Information). Comparing the tested photocatalysts,  $\text{Nb-BiVO}_4$  exhibits the best photodegradation efficiency with a removal of 72% of RhB after 180 min irradiation. Such performance is due to the beneficial morphology of the film surface that exhibits high porosity and thus higher active surface area than the other materials (Fig. 1). Both composites exhibit also excellent photooxidative properties by degrading from 56 to 61% of pollutants which is better than the single components (Fig. 2a). It means that composites are constituted of efficient heterojunction between titania and bismuth vanadate that improves electron-hole pair separation and transport within the material: photogenerated  $e^-$  are accumulated in  $\text{TiO}_2$  while  $h^+$  are concentrated in  $\text{BiVO}_4$ .<sup>13</sup> It is also noteworthy that top- $\text{TiO}_2/\text{BiVO}_4$  is more efficient than top- $\text{BiVO}_4/\text{TiO}_2$  (Fig. 2a). The photocatalytic mechanism was evaluated using different charge carriers (Fig. 2b).

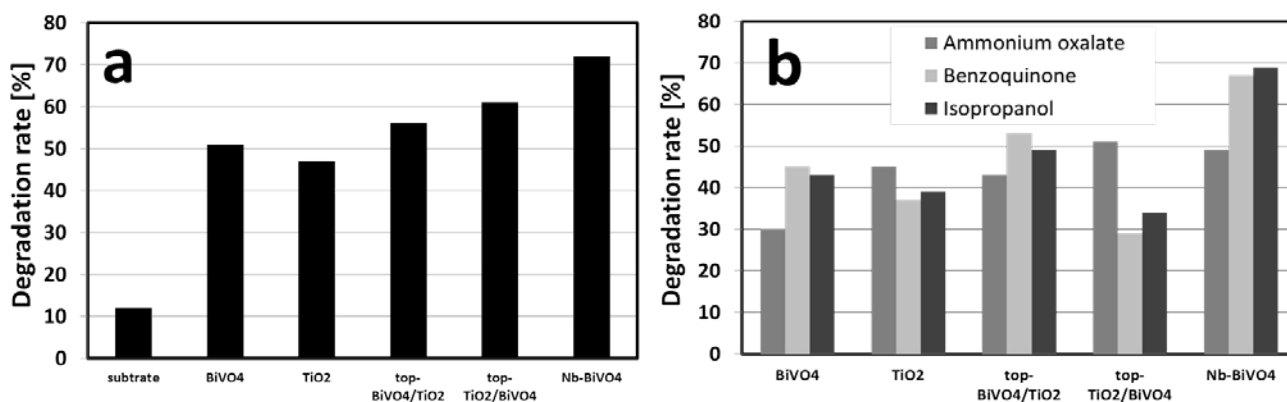


**Figure 2.** (a) Degradation rates of RhB after 180 min irradiation under solar-like light and (b) the corresponding effects of charge scavengers on the removal efficiencies of RhB.

It is obvious that photocatalytic degradation proceeds mainly through photogenerated holes using films exhibiting BiVO<sub>4</sub>-based material at their surface (i.e. pristine BiVO<sub>4</sub>, Nb-BiVO<sub>4</sub> and top-BiVO<sub>4</sub>/TiO<sub>2</sub> composite) while films with titania at the surface oxidize essentially through superoxide and hydroxyl radicals. Indeed, the photocatalytic activity of top-TiO<sub>2</sub>/BiVO<sub>4</sub> and pure TiO<sub>2</sub> is strongly inhibited in presence of O<sub>2</sub><sup>•-</sup> and OH<sup>•</sup> scavengers indicating that they are the main oxidative species (Fig. 2b). Similarly, the other photocatalysts show a strong decrease in photooxidative degradation rate of RhB in presence of ammonium oxalate which are thus the main reactive species in this case (Fig. 2b).

The antimicrobial properties of BiVO<sub>4</sub>-based films are summarized in Fig. 3 after simulated solar irradiation and in the dark. It is clear that in absence of light, the series of BiVO<sub>4</sub>-based photocatalysts are not able to inactivate the MRSA strain (Fig. 3a). There is also no photolysis of bacterial cells under irradiation alone. Under our conditions, 30 min irradiation time is too short to put in evidence any antimicrobial effect (Fig. 3b). On the other hand, after 60 min irradiation (Fig. 3b), Nb-BiVO<sub>4</sub> and top-BiVO<sub>4</sub>/TiO<sub>2</sub> composite exhibit significant photo-induced antimicrobial properties (43 and 39% inactivation, respectively) while the remaining samples show poor bactericidal activity. It is remarkable that, in case of top-TiO<sub>2</sub>/BiVO<sub>4</sub> composite, only weak photo-disinfectant properties are observed although this composite has good photooxidative power with the production of superoxide and hydroxyl radicals. So far, we cannot explain this observation. But it could be assumed that inactivation of the bacterial strains depends not only on the degradation mechanism but also on other factors related to the bacterial cell such as its wall structure. Thus it is probable that the affinity of MRSA is higher toward BiVO<sub>4</sub> surface than titania surface.

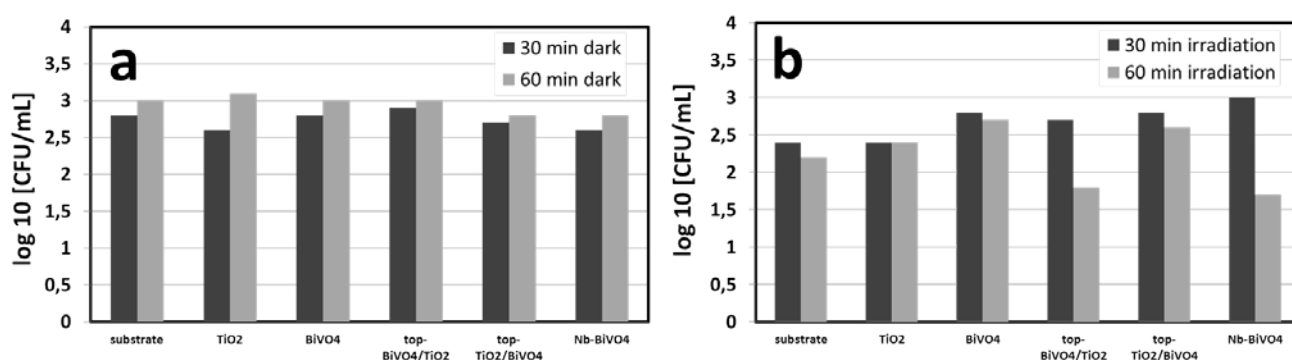


**Figure 3.** Survival of MRSA strain on the different BiVO<sub>4</sub>-based materials (a) in the dark, (b) after 30 and 60min solar-like irradiation.

In our case, the two antimicrobial active samples (Nb-BiVO<sub>4</sub> and top-BiVO<sub>4</sub>/TiO<sub>2</sub>) exhibit a photocatalytic power through holes and their bactericidal activity improves by the fact that (1) Nb-BiVO<sub>4</sub> film exhibits porous structure with high surface area (Fig. 1c) and (2) top-BiVO<sub>4</sub>/TiO<sub>2</sub> composite has

improved electron-hole pair separation giving rise to increased lifetime of holes.<sup>14</sup> In addition it has been reported that photogenerated holes from BiVO<sub>4</sub> can act as efficient oxidative agents toward bacterial cells if close contact between the photocatalyst and the bacteria is achieved.<sup>18,23,24</sup> Therefore from the above discussion, it could be assumed that the high antimicrobial activity of Nb-BiVO<sub>4</sub> is the result of fulfilled conditions for an efficient attack of the cell membrane by photogenerated holes: high surface area combined with good affinity of MRSA at bismuth vanadate photocatalyst surface.

## Conclusion

Different supported BiVO<sub>4</sub>-based materials in the form of films were tested in both the photocatalytic degradation of RhB and the inactivation of MRSA strain under simulated solar irradiation. It was found that the best material was Nb-BiVO<sub>4</sub> due to its beneficial morphology which results in high degradation of pollutant and substantial bacterial inactivation. The mechanism of photo-induced properties using Nb-BiVO<sub>4</sub> involved directly the photogenerated holes. It is the first time that both photocatalytic and antimicrobial activities of different supported BiVO<sub>4</sub> systems are simultaneously reported under the same conditions, especially for the inactivation of clinically important MRSA which achieves here 43% in presence of Nb-modified BiVO<sub>4</sub>.

## Conflicts of interest

There are no conflicts to declare.

## Acknowledgements

Authors wish to acknowledge the financial supports granted by the Scientific Grant Agency of the Slovak Republic and the Statutory Research of the Wroclaw Medical University through the projects VEGA 1/0276/15 and ST.A130.16.032, respectively. Authors gratefully thank Tomas Roch for XRD measurements. This work was also supported by the Research and Development Operational Program funded by the ERDF (project ITMS:26240220027).

## References

- 1 Y. Park, K.J. McDonald and K.S. Choi, *Chemical Society Reviews*, 2013, **42**, 2321.
- 2 K.R. Tolod, S. Hernandez and N. Russo, *Catalysts*, 2017, **7**, 13.
- 3 X. Lin, D. Xu, Y. Xi, R. Zhao, L. Zhao, M. Song, H. Zhai, G. Che and L. Chang, *Colloids and Surfaces A: Physicochemical and Engineering Aspects*, 2017, **513**, 117-124.
- 4 X. Lin, Y. Xi, R. Zhao, J. Shi and N. Yan, *RSC Advances*, 2017, **7**, 53847-53854.

- 5 X. Lin, D. Xu, S. Jiang, F. Xie, M. Song, H. Zhai, L. Zhao, G. Che and L. Chang, *Catalysis Communications*, 2017, **89**, 96-99.
- 6 X. Lin, D. Xu, R. Zhao, Y. Xi, L. Zhao, M. Song, H. Zhai, G. Che and L. Chang, *Separation and Purification Technology*, 2017, **178**, 163-168.
- 7 Y. Kanigaridou, A. Petala, Z. Frontistis, M. Antonopoulou, M. Solakidou, I. Konstantinou, Y. Deligiannakis, D. Mantzavinos and D.I. Kondarides, *Chemical Engineering Journal*, 2017, **318**, 39.
- 8 Y. Liu, J. Kong, J. Yuan, W. Zhao, X. Zhu, C. Sun and J. Xie, *Chemical Engineering Journal*, 2018, **331**, 242.
- 9 T. Saison, N. Chemin, C. Chaneac, O. Durupthy, L. Mariey, F. Mauge, V. Brezova and J.P. Jolivet, *Journal of Physical Chemistry*, 2015, **119**, 12967.
- 10 K. Zhang, Y. Liu, J. Deng, S. Xie, X. Zhao, J. Yang, Z. Han and H. Dai, *Applied Catalysis B: Environmental*, 2018, **224**, 350.
- 11 T. Huo, X. Zhang, X. Dong, X. Zhang, C. Ma, G. Wang, H. Ma and M. Xue, *Journal of Materials Chemistry A*, 2014, **2**, 17366.
- 12 U. Lamdab, K. Wetchakun, S. Phanichphant, W. Kangwansupamonkon and N. Wetchakun, *Catalysis Today*, 2016, **278**, 291.
- 13 O. Monfort, T. Roch, M. Gregor, L. Satrapinskyy, D. Raptis, P. Lianos and G. Plesch, *Journal of Environmental Chemical Engineering*, 2017, **5**, 5143.
- 14 O. Monfort, S. Sfaelou, L. Satrapinskyy, T. Plecenik, T. Roch, G. Plesch and P. Lianos, *Catalysis Today*, 2017, **280**, 51.
- 15 G. Odling, and N. Robertson, *ChemPhysChem*, 2016, **17**, 2872.
- 16 A.O. Ibhaddon and P. Fitzpatrick, *Catalysts*, 2013, **3**, 189.
- 17 C. Adan, J. Marugan, S. Obregon and G. Colon, *Applied Catalysis A: General*, 2016, **526**, 126.
- 18 C. Adan, J. Marugan, S. Obregon and G. Colon, *Catalysis Today*, 2015, **240**, 93.
- 19 A.Y. Booshehri, S.C.K. Goh, J. Hong, R. Jiang and R. Xu, *Journal of Materials Chemistry A*, 2014, **2**, 6209.
- 20 P. Ganguly, C. Byrne, A. Breen and S.C. Pillai, *Applied Catalysis B: Environmental*, 2018, **225**, 51.
- 21 C.K. Huang, T. Wu, C.W. Huang, C.Y. Lai, M.Y. Wu and Y.W. Lin, *Applied Surface Science*, 2017, **399**, 10.
- 22 C. Regmi, Y.K. Kshetri, T.H. Kim, R.P. Pandey and S.W. Lee, *Molecular Catalysis*, 2017, **432**, 220.
- 23 R. Sharma, Uma, S. Singh, A. Verma and M. Khanuja, *Journal of Photochemistry and Photobiology B: Biology*, 2016, **162**, 266.
- 24 W. Wang, Y. Yu, T. An, G. Li, H.Y. Yip, J.C. Yu and P.K. Wong, *Environmental Science & Technology*, 2012, **46**, 4599.
- 25 Z. Xiang, Y. Wang, P. Ju, Y. Long and D. Zhang, *Journal of Alloys and Compounds*, 2017, **721**, 622.
- 26 Z. Xiang, Y. Wang, D. Zhang and P. Ju, *Journal of Industrial and Engineering Chemistry*, 2016, **40**, 83.
- 27 S.J. Dancer, *Lancet Infectious Diseases*, 2008, **8**, 101.